BioSense/SR-BioSpectra, Demonstrations of Wide Area/Early Warning for Bioaerosol Threats: Program Description and Early Test and Evaluation Results

Jean-Robert Simard[*a], Sylvie Buteau[a], Pierre Lahaie[a], Pierre Mathieu[a], Gilles Roy[a], Denis Nadeau[a], John McFee[b], Jim Ho[b], Susan Rowsell[b]

Nicolas Hô[c], François Babin[c], Daniel Cantin[c], Dave Healey[d], Jennifer Robinson[d], Scott Wood[d], Jack Hsu[d]

[a]DRDC Valcartier, 2459, boul. Pie-XI North, Val-Bélair, Qc, Canada G3J 1X5
[b]DRDC Suffield, Box 4000, Medicine Hat, AB, Canada T1A 8K6
[c]INO, 2740, rue Einstein, Quebec City, Quebec, CANADA G1P 4S4
[d]MDA, 13800 Commerce Parkway, Richmond, British Columbia, Canada V6V 2J3

ABSTRACT

Threats associated with bioaerosol weapons have been around for several decades and have been mostly associated with terrorist activities or rogue nations. Up to the turn of the millennium, defence concepts against such menaces relied mainly on point or in-situ detection technologies. Over the last 10 years, significant efforts have been deployed by multiple countries to supplement the limited spatial coverage of a network of one or more point bio-detectors using lidar technology. The addition of such technology makes it possible to detect within seconds suspect aerosol clouds over area of several tens of square kilometers and track their trajectories. These additional capabilities are paramount in directing presumptive ID missions, mapping hazardous areas, establishing efficient counter-measures and supporting subsequent forensic investigations. In order to develop such capabilities, Defence Research and Development Canada (DRDC) and the Chemical, Biological, Radiological-Nuclear, and Explosives Research and Technology Initiative (CRTI) have supported two major demonstrations based on spectrally resolved Laser Induced Fluorescence (LIF) lidar: BioSense, aimed at defence military missions in wide open spaces, and SR-BioSpectra, aimed at surveillance of enclosed or semi-enclosed wide spaces common to defence and public security missions. This article first reviews briefly the modeling behind these demonstration concepts. Second, the lidar-adapted and the benchtop bioaerosol LIF chambers (BSL1), developed to challenge the constructed detection systems and to accelerate the population of the library of spectral LIF properties of bioaerosols and interferents of interest, will be described. Next, the most recent test and evaluation (T&E) results obtained with SR-BioSpectra and BioSense are reported. Finally, a brief discussion stating the way ahead for a complete defence suite is provided.

Keywords: bioaerosol, standoff, detection, classification, chamber, calibration, spectral, LIF.

1. INTRODUCTION

Over three decades, significant efforts from multiple countries have been undertaken to develop new defence capabilities against aerosolized biological threats over wide areas. These efforts have focused on providing answers to three main questions: where the threat is, when it was detected and what type of biological threat it is. The first objective is to obtain the location of such threats within a few meters over a monitored area that may be several tens to a hundred square kilometers. Since aerosols may travel as fast as the wind, such aerosolized bio-threats must be detected within seconds and be tracked to identify contaminated areas (and people). Finally, it is paramount to confirm the presence and the type of biological threats detected in order to deploy initial mitigating actions, including the appropriate medical counter

[*] Jean-Robert.Simard@drdc-rddc.gc.ca; phone 1-418-844-4000, x4128;fax 1-418-844-4511; www.drdc-rddc.gc.ca

measures. Furthermore, a successful forensic investigation following such event will greatly depend on the quality of the information answering these three questions.

Over the years, lidar has proven to be the most promising technology in providing valuable answers to the three questions discussed in the previous paragraph. Single long-range lidars can provide standoff detection and tracking capabilities for operational scenarios involving sufficiently long line-of-sights. Short-range lidars, when networked, can provide efficient surveillance of enclosed, semi-enclosed, or even open wide area venues involving line-of-sights of several tens or even hundreds of meters. Both lidar types can provide excellent information concerning the location of a threatening cloud as a function of time. However, to obtain answers within seconds concerning what is the type of the suspected bioaerosol threat with an acceptable probability of detection and associated false alarm rate, special lidar technologies have been developed. All of these special lidars developed to better answer the 'what' question exploit one or more of three main multi-spectral technologies: spectrally resolved laser induced fluorescence, multi-wavelength depolarization ratios and differential scattering (DISC). Multi-wavelength depolarization and DISC exploit the optical elastic scattering properties of the air-aerosol interface (mainly the complex refractive index step and aerosol shape), which are sometimes referred to as extrinsic properties. The spectrally resolved LIF exploits the fluorescence of different chemical centers distributed within the aerosols, which are sometimes referred as intrinsic properties. Contrary to depolarization and DISC, it is believed spectrally resolved LIF can provide better quality information because it is not (or at least much less) affected by the ambient moisture level that varies the water film thickness at the air-aerosol interface. However, the depolarization and DISC approaches have valuable advantages such as exploiting a much higher aerosol cross section (equivalent to requiring a much smaller, less radiometrically powerful lidar for similar detection ranges or aerosol concentrations) and similar sensitivities between day and night.

This paper describes the efforts conducted over the last five years by the government of Canada in partnership with private industry to demonstrate eye/skin safe spectrally resolved LIF/SWIR (short wave infrared) scanning/classifying lidar devices capable within seconds of detecting, mapping, tracking and classifying bioaerosol threats over a wide area. First, an overview of the multi-wavelength lidar modeling used throughout this effort is described. Next, the supporting assets (lidar-adapted/benchtop bioaerosol chambers and calibrated LIF targets) needed to characterize/evaluate the developed lidar systems are discussed. Then, the long (BioSense) and short (SR-BioSpectra) range spectrally resolved LIF lidar systems are described. Finally, a conclusion is provided.

2. MODELING

In order to provide a sound direction for the development of a standoff biodetection program, it is paramount to build a detailed model to better our understanding of the relevant phenomenology and help in the identification of the technical challenges. Early within the DRDC standoff biodetection program, we derived a working model based on the analysis provided by Measures[1]. This section reviews how we adapt the general lidar principles found in this reference to our specific needs.

The fundamental differential lidar equation below describes the spectral element of optical electromagnetic (light) power dP_λ at wavelength λ detected at time t resulting from elastic or inelastic scattered light, induced with an excitation wavelength λ_0, from a volume element dV located at a position $\vec{r}$. In this equation, J_λ is defined as the spectral radiance induced in that volume element and p_λ as the fraction of that radiance reaching the lidar detector.

$$dP_\lambda(\lambda_0, \vec{r}, t) = J_\lambda(\lambda_0, \vec{r}, t)\, p_\lambda(\vec{r})\, dV \tag{1}$$

By inserting the detailed expressions for the induced spectral radiance J_λ and for the fraction of this induced radiance detected p_λ, and solving the resulting equation while taking into account the time delay associated with the light travelling between the sensor location and the probed volume, as well as a several simplifying approximations (a detailed description of this solution is in Simard[2]), equation 1 leads to

$$E_\lambda^i(\lambda_0, R_0, \Delta R) = \underbrace{n_p E_L}_{\text{laser energy}}\ \underbrace{\xi_\infty \frac{A_{AS}}{R_0^2}}_{\text{geometry}}\ \underbrace{t_{\lambda_0}^a(R_0)\, t_\lambda^a(R_0)}_{\text{atmospherics}}\ \underbrace{t_{\lambda_0}^e t_\lambda^c}_{\text{optics}}\ \underbrace{\Delta R\, N_i}_{\text{cloud column}}\ \underbrace{\sigma_\lambda^i(\lambda_0)}_{\text{scatterers}}\ . \tag{2}$$

Here is the spectral light signal incident on the lidar detector following scattering of excitation light at wavelength λ_0 by scatterers i located within the range interval ΔR at range R_0. This equation has the advantage of modeling the signal collected as a function of the laser energy sent to the probed cell (n_p is the number of binned laser pulses and E_L is the energy per laser pulse), the collection geometry (A_{AS} is the area of the lidar collector aperture stop and ξ_∞ is the overlap factor at large ranges defining the fraction of the signal collected that will reach the lidar detector), the atmosphere (and are the atmospheric transmission between the sensor and the probed cell at the emitted and collected laser wavelengths, respectively), the lidar optics (and are the transmission of the lidar emitter and collector optics, respectively), the probed cloud column of aerosol species i (N_i is the concentration of aerosol i) and the scattering properties of species i (being the spectral cross section of aerosol species i when irradiated at wavelength λ_0). This form of the inelastic lidar equation is particularly useful for the special case of spectrally resolved LIF lidar which is one of the two phenomenologies exploited by the DRDC standoff biodetection program reported here (the other being classical elastic scattering lidar cloud mapping).

Equation 2 describes the spectrally distributed scattering from scatterers of type i collected from the probed volume. However, more than a single type of inelastic scatterer may be present in that volume. This can be taken into account by expressing the collected spectrum as a linear combination of scattering spectra, each originating from different scatterers present in the probed volume,

$$\overrightarrow{E_\lambda} = E_1 \overrightarrow{s_\lambda^1} + E_2 \overrightarrow{s_\lambda^2} + \cdots + E_{N2} \overrightarrow{s_\lambda^{N2}} + E_{H2O} \overrightarrow{s_\lambda^{H2O}} + \cdots . \tag{3}$$

In this last equation, each linear term is a simplified representation of equation 2 where are the instrument-uncorrected spectral bases formed from the combination of the spectral variables associated with species i, the atmosphere and the optics, subsequently normalized by the modulus, and E_i combines all scalar variables of equation 2 plus the normalization factor used to define . Also, the inelastic Raman scattering originating from atmospheric nitrogen and water has been introduced in equation 2 as examples of environmental inelastic scatterers. It is important to observe that, unless the spectral transmissions of the atmosphere and the lidar collector are known, the library of bases will be environment/hardware-dependent.

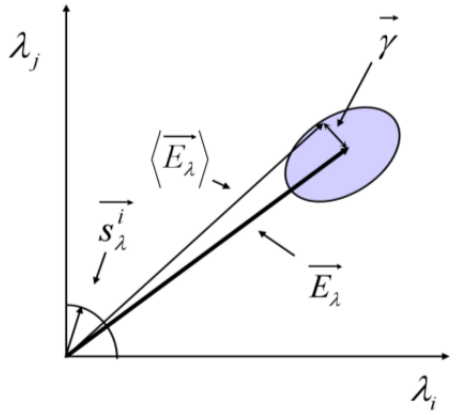

Figure 1 Schematic representation of the multidimensional Euclidian spectral analysis space. In this space, each axis reports the amplitude of a spectrum at a given wavelength λ_i. is the spectrum collected with the inelastic lidar, is the spectrum built from the library of bases following equation 3 after applying a best fit (in the least squares sense) with . is the quality of fit parameter resulting from the least squares fit procedure. This latter parameter, also defined as the multi-dimensional Euclidian distance between the two spectra, is closely related to the Mahalanobis distance once the statistical properties of the problem associated with equation 3 are inserted. Also in this figure, is the normalized member i derived from the library of known spectra.

Equation 3 defines a multivariate linear problem where each normalized spectral basis is constant for a given species (and a given environment and lidar) and where the amplitude E_i is the variable reporting the combined scalar parameters

of equation 2 including the concentration N_i, the quantum yield and the size of the aerosol species i, the last two being parts of the scatterer cross section .

Figure 1 is a schematic representation of the spectral classification problem associated with equation 3 in the multi-spectral Euclidian space where each axis of this space is the amplitude of a spectrum at a given wavelength λ_i. In this model, is the spectrum built from the library of bases following equation 3 that best fits (in the least square sense) the collected spectrum . The exploitation of the classification information from this multivariate analysis can be derived by monitoring the coefficients E_i (associated with species i in equation 3) or by applying thresholds on the quality of fit parameter for a given combination of bases, both after applying a least squares fitting procedure. The latter, once the statistics (mean and covariance) of the parameteric part of equation 3 are inserted, opens the door to a powerful classification tool, the Mahalanobis distance. The Mahalanobis distance has the advantage of normalizing the Euclidian distance between the two spectra with respect to the covariance (essentially a multivariate standard deviation) of the measured phenomenon, providing a probabilistic assessment of the classification result.

BioSense and SR-BioSpectra, the two standoff biodetection systems described in sub-sections 4.1 and 4.2, integrate a classification algorithm largely based on this Mahalanobis distance concept.

3. DEVELOPED SUPPORTING ASSETS

In order to support the development of new capabilities in standoff biodetection, two well instrumented bioaerosol chambers have been built. In addition, to facilitate the transfer of information obtained with these chambers while challenging different spectrally resolved LIF lidar systems, calibration targets have been specially designed. These assets are briefly described in the following three sub-sections.

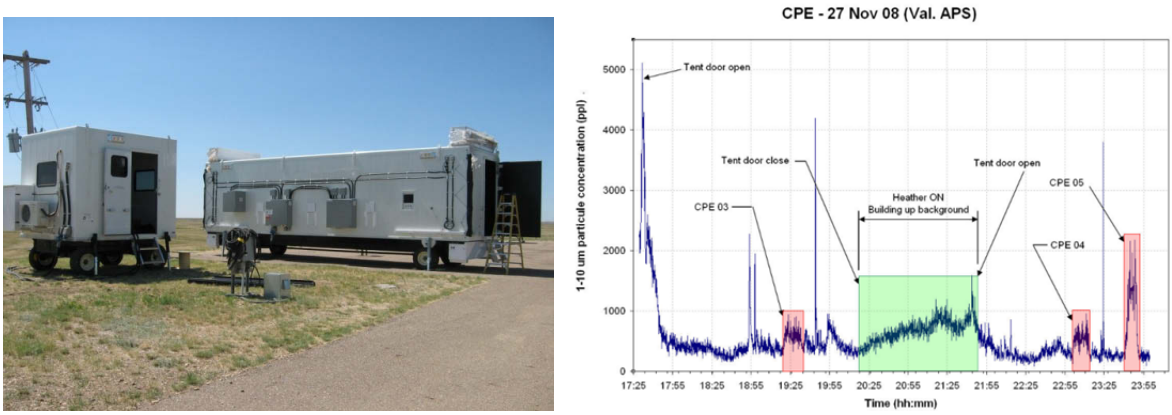

Figure 2 Photograph of the well instrumented lidar-adapted bioaerosol chamber (left) developed under the BioSense project. This asset includes a 40-foot long trailer where challenge clouds are confined between two vertical air curtains and the smaller control trailer that regulates its concentration. It also referees aerosol clouds using an Aerodynamic Particle Sizer or APS (reporting the concentration in ppl as well as their aerodynamic size distribution), a slit sampler array (providing ACPLA), a high volume liquid impinger (assessing pfu/l and µg/l) and a Compact-FLuorescent Aerosol Particle Sensor or C-FLAPS (reporting the % of fluorescing aerosols). The graphic at the right shows the concentration of aerosols in the chamber as measured by the APS as a function of time. The three pink boxes show 2 releases of clouds of BG having about 100 ACPLA (CPE 03 and 04) and the maximum controlled BG cloud concentration achievable at that time (CPE 05). The green box reports the background aerosol buildup during chamber heating. Note that this trial was held under freezing temperatures while housing the 40-foot long trailer in a Weatherhaven Tent (not shown in the picture).

3.1 Lidar-adapted bioaerosol chamber

This chamber was built to challenge short and long range standoff biodetection systems in a realistic environment. It is composed of a 40-foot (~12 m) trailer, where disseminated aerosol clouds are confined between two air curtains, and a chamber control unit (see Fig.2). The use of air curtains and large doors at each end provides a 10-m-long probed volume having a cross section of about 2 m x 2 m free of solid obstacles. These design choices make such a chamber

well suited to challenge standoff biodetection systems located at ranges of a few tens of meters up to a few kilometers depending on the lidar's optical divergence and pointing accuracy/stability.

The biological aerosol is produced from a wet solution using sprayers based on ultrasonic (Sono-Tek) or mechanical blower technology (Micronair). The concentration of the bioaerosol cloud is controlled through a feedback loop from measurements provided by a C-FLAPS sampling the probed volume. We are presently extending the capability of the chamber to produce bioaerosol clouds from solid powders. The chamber has been instrumented to produce well characterized clouds of *Bacillus atrophaeus* (BG), a spore bacterial simulant; *Erwinia* herbicola (EH), a vegetative bacterial simulant; ovalbumin (OVA), a toxin simulant; and the bacteriophage MS2, a virus simulant. The chamber produces challenge bacterial clouds with stabilized concentrations of a few tens up to about 100 Agent Containing Particles per Liter of Air (or ACPLA) of BG and EH. These types of clouds are refereed using a slit sampler array. The concentration challenge produced with clouds of OVA is of the order of a microgram per liter of air (µg/l) refereed with a High volume liquid impinger (XMX/2L-102, Dycor Technologies). The concentration challenge produced with clouds of MS2 is about 1000 plaque forming units per liter of air (pfu/l) refereed also with the XMX/2L-102.

This lidar-adapted bioaerosol chamber has been deployed to evaluate the sensitivity of SR-BioSpectra (see subsection 4.1) and will be deployed to evaluate BioSense (see section 4.2).

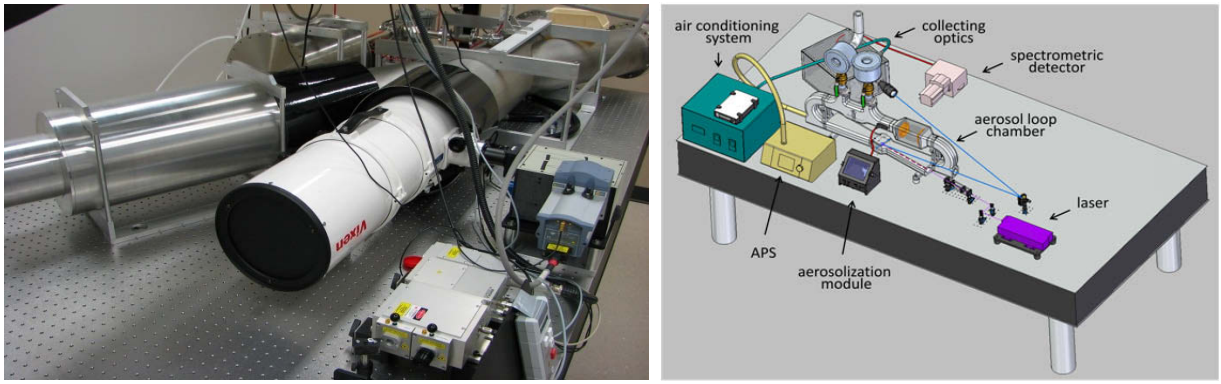

Figure 3 Picture of the benchtop bioaerosol LIF chamber (left) developed to improve the understanding of the spectral LIF properties of aerosols and accelerate the buildup of a library of aerosol spectral fluorescent properties. It is designed as a collector axis crossing the emitter axis defining an effective probed volume. Aerosols of interest are injected in this volume and the produced inelastic scattering is collected and directed into a highly sensitive spectrometric detector. A second generation chamber is presently being constructed (right). This chamber is expected to provide much higher sensitivity as well as much better control of the aerosol clouds under investigation.

3.2 Benchtop bioaerosol LIF chamber

The benchtop bioaerosol LIF chamber, a Biohazard Security Level 1 (BSL1) asset, has been developed to accelerate the construction of the library of spectral properties of aerosols of interest (including simulants of biological agents) and further our understanding on how these spectral properties can be affected by the methods of production or growth of these aerosols as well as the aerosolization techniques.

The main advantages of such a chamber are the much reduced overhead in terms of time and money, as well as a much better control of the experimental environment when compared with a long range outdoor measurement campaign involving assets like the lidar-adapted bioaerosol chamber.

A first chamber, designed in collaboration with Laval University, is shown in Fig.3. This design is composed of an emitter and a collector in a 26-degree cross axis configuration. This cross axis has the advantage of providing a much better control of parasitic light returns that do not originate from aerosol scattering.

In this design, the emitter first expands a pulsed (200 Hz pulse repetition frequency or PRF) 355 nm ultraviolet (UV) laser beam to a final diameter of about 190 mm. The beam then crosses an effective probed volume of about 18 liters where scattering from aerosols is collected with a 10-inch (~254 mm) Newtonian telescope and directed into a spectrometer. At the exit window of the spectrometer, an intensified charge coupled device (ICCD) collects the spectrum (380 to 775 nm span with a resolution of about 4 nm) produced by each laser pulse. These spectra are binned on the

camera chip for a period of about 20 seconds before being read out and stored in a computer. This readout cycle is repeated for a period of up to 20 minutes during which the aerosols of interest are injected in the probed volume. These aerosols are injected from a dry powder using a custom venturi device and a series of mixing fans. An APS records the concentration and size distribution of the aerosol in the probed chamber for the duration of the acquisition. A complete description of this chamber and associated instruments has been produced by Déry[3].

Since its delivery at DRDC Valcartier, multiple campaigns of measurements with different types of biological materials have been performed with this benchtop bioaerosol LIF chamber. Probably the most instructive of these campaigns was the one investigating the effect of the growth media on the normalized spectral LIF signatures of *Bacillus atrophaeus*, *Bacillus thuringiensis* and *Erwinia herbicola* (all in vegetative state). Laflamme[4] has not only shown that the selected growth media will affect the resulting LIF signatures but also that the signatures for a bacteria in its broth, the broth alone as well as the triple-washed bacteria have all distinct and repeatable spectral signatures.

Built on the lessons learned from the work done with this benchtop bioaerosol LIF chamber, we are presently in the process of building a second generation chamber. This second chamber design (shown in Fig.3), that we have named Biosafety Level 1 LIF Bench top Bioaerosol Chamber (BSL1 LIF BBC), is expected to provide a much higher radiometric sensitivity and, a better control of the aerosolized materials, the air temperature and relative humidity. It is based on a loop configuration that may be closed or open to assess aerosol bleaching properties.

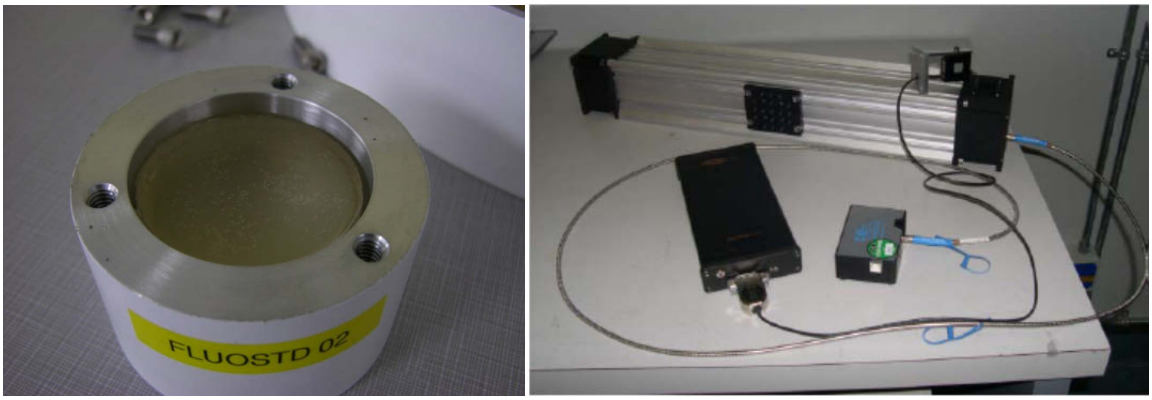

Figure 4 Picture of a calibration LIF target (left) and the optical setup (right) used to derive precisely the quantum yield of a calibration target as well as its spectral probability distribution.

3.3 Calibrated LIF targets

In order to efficiently develop a standoff biodetection capability, it is essential to build a spectral library of aerosol LIF properties independent of the measurement instruments. This is necessary to facilitate the transfer of the properties determined by the benchtop bioaerosol LIF chamber to a given standoff biodetection system (and between different lidar systems) and to implement spectral corrections for the transmission of the atmosphere .

The concept of use of these calibrated targets is to first acquire the signal from the targets with the lidar system which is later to be challenged with aerosols of interest. From this preliminary calibration acquisition, the spectral response of the lidar system (mainly related to in equation 2) is assessed. This calibration measurement should be acquired at a sufficiently short range to be able to neglect the effect of the atmospheric transmission or at a range for which the atmospheric spectral transmission is known. For optimum calibration using the LIF targets, in addition to knowing precisely their fluorescent quantum yields and spectral probability function, it is highly desirable that the spectral probability function have no values which are near to zero in the wavelength interval of interest (380-700 nm). If such targets provide little or no fluorescence in portions of the spectrum, calibration in these parts will yield a poor signal-to-noise ratio (S/N) or simply be infeasible. To achieve these desirable properties, we have fabricated the calibration targets using a mixture of quantum dots and a short wavelength fluorescent organic dye, the two being diluted in a polyurethane matrix. Before use, these targets first need pre-bleaching to achieve an acceptable photo-stability. In addition, to maximize the precision of the calibration procedure, the calibrated fluorescence spectral efficiency of these targets are derived with a dedicated optical setup shortly (a few hours or less) before being probed by the lidar of interest. Figure 4 shows a picture of a calibrated fluorescent target (left) and this dedicated optical setup (right). This optical calibration setup is composed of: a fiber-coupled low power CW UV laser (355 nm), a miniature fiber-coupled spectrometer, a fixed

optical enclosure with appropriate ports for the LIF target to be calibrated, the optical fibers (emission and collection) and a power meter. After the calibration of this setup with an irradiance calibration lamp, the fluorescence efficiency of the calibration target is derived from radiometric analysis.

Once calibrated with the dedicated setup, the LIF calibration targets are probed with the spectrally resolved UV LIF lidars before and/or after these lidars are challenged with specific aerosol clouds of interest. Starting from the model described in section 2 and using the calibration target fluorescence efficiency previously measured, the spectral cross section of the aerosol species is derived from the following equation,

$$\sigma_{\lambda}^{i}(\lambda_0) = \frac{1}{\Delta R\, N_i} \frac{\gamma (n_p E_L)_{cal}}{(n_p E_L)} \left(\frac{R_0}{R_{cal}} \right)^2 \frac{\xi_{cal}}{\xi_{\infty}} \kappa_{\lambda}(\lambda_0) \frac{E_{\lambda}^{i}}{E_{\lambda}^{cal}}, \tag{4}$$

where quantities having the index '*cal*' refer to parameters associated with the calibration target measurement and where γ is the fraction of the lidar energy incident on that target during this calibration procedure. A similar equation was developed for calibrated measurements with the Biosafety Level 1 LIF Bench top Bioaerosol Chamber.

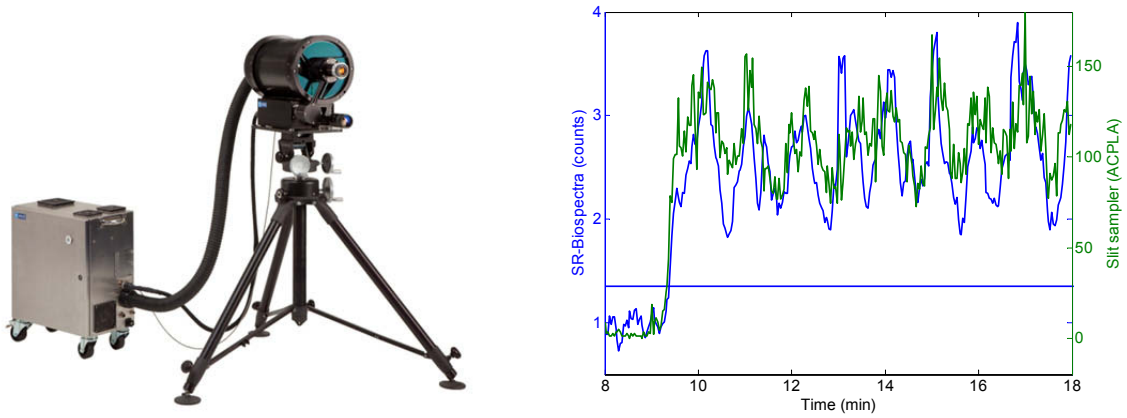

Figure 5 Picture of the SR-BioSpectra beta model (left). The optical module, composed of an 8-inch (~203 mm) collecting telescope placed above a frequency-tripled Nd-YAG laser source, is shown on a tripod. It is connected to the optoelectronic enclosure via optical fibers. The graph at the right shows a typical sensitivity result obtained with SR-BioSpectra at night during a BG release (3 µm average diameter with a probed volume 10 m long) at a range of 100 m during the first phase of the SR-BioSpectra beta T&E. The left y axis shows the averaged number of detected counts per laser pulse binned over a 10-sec time interval and over the PMT array as a function of the time of the trial (blue trace). The right axis shows the output of the referee sensor (green trace) in ACPLA provided by a slit sampler array for the same time period. Based on the correlation between the two traces and the statistics of the SR-BioSpectra outputs before the dissemination, the sensitivity at 4 times the standard deviation is calculated to be better than 40 ACPLA (25% ACPLA/ppl ratio).

4. BIOAEROSOL THREAT WIDE AREA/EARLY WARNING SYSTEMS

Two systems have been developed to demonstrate the concepts associated with the wide area/early warning for the presence of bio-aerosolized threats. These two eye/skin-safe systems have resulted from the lessons learned with the Standoff INtegrated Biological Active Hyperspectral Detection (SINBAHD) investigation project, sponsored by DRDC from 1999-2002, that reported the feasibility of spectrally resolved LIF lidars for the standoff detection and classification of aerosolized biological threats[5]. The first system, SR-BioSpectra, is a short-range (SR) lidar with command and control (C2) networking capabilities providing operational capabilities in surveillance, alerting and warning for the presence of bio-threats over indoor, semi-enclosed and outdoor venues. It was developed between 2007 and 2010 as a Technology Demonstration (TD) with 66% funding from the Chemical, Biological, Radiological-Nuclear, and Explosives (CBRNE) Research and Technology Initiative (CRTI) of the Canadian government. The other part of the funding originated directly from the project partners: INO, MDA, DRDC Suffield and DRDC Valcartier. The second system, BioSense, is a long range (up to 5 km) standoff bioaerosol sensing, mapping, tracking, and classifying

system. It has been under development since 2006 under the Technology Demonstration Program of DRDC. The next 2 subsections provide an overview of these 2 systems.

4.1 SR-BioSpectra

SR-Biospectra is a short range spectrally resolved LIF lidar system designed to demonstrate that such technology can be sufficiently compact and inexpensive to provide within seconds, when networked under a single control station, an efficient surveillance and alert status for the presence of aerosolized biological threats over stadiums, malls, airports, harbours and other sites that attract large populations over a wide area.

This demonstrator was built in two phases (alpha and beta). The beta model resulting from this effort (shown in figure 5) is based on a versatile 2-module approach: the optical head and the optoelectronic enclosure. The optical head is composed of an 8-inch (~203 mm) collecting telescope, a 1 kHz PRF Nd-YAG laser with the third-harmonic frequency conversion module producing 100 µJ pulses at 355 nm and the emitter optics that expands the laser beam and aligns it with the collector optical axis. The optoelectronic enclosure houses the laser light source pump (based on a stack of laser diodes), a spectrometer, an array of 32 photomultiplier tubes and a core computer. The two modules are essentially interconnected with optical fibers: a fiber bundle carrying the collected optical signal from the telescope to the spectrometer and a fiber conveying the laser pump light from the diode stack to the Nd-YAG laser module. The core computer software controls the electronic peripherals during an acquisition as well as the detection and classification algorithms. It can also interface, via an Ethernet link, with a remote client hosting the command and control (C&C) software. The C&C software can configure the core computer or multiple computers in three modes of operation: manual or automatic surveillance, or signature acquisition. This may be done using a graphical overlay of the site under surveillance where each core computer and air volumes probed by the corresponding optical heads are shown graphically as nodes with different alert status.

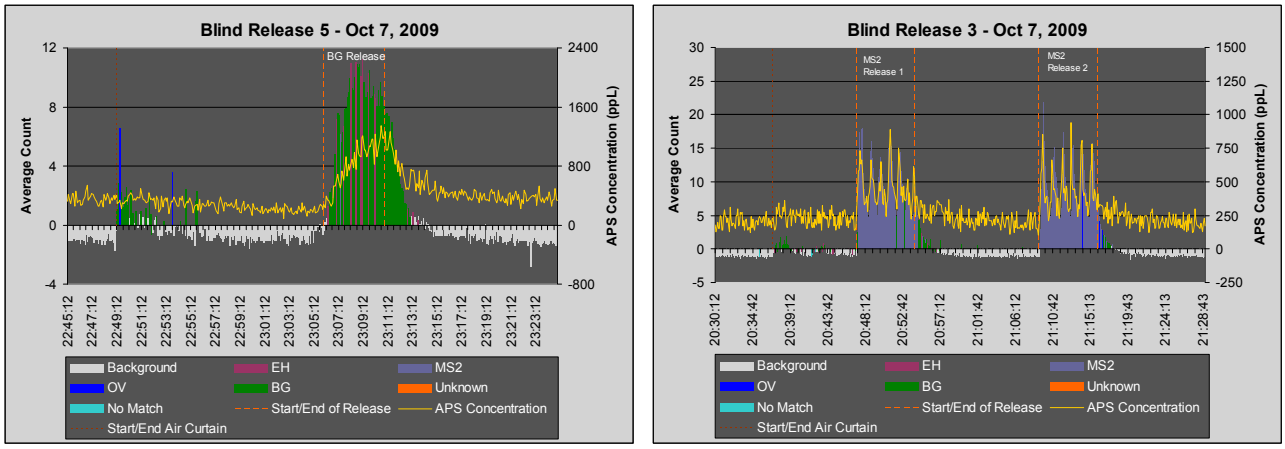

Figure 6 Two examples from blind runs made with SR-BioSpectra while challenged with the lidar-adapted bioaerosol chamber (10-m long cloud) from a range of 100 m. The upper windows of each picture show the time evolution of the classification performed by the instrument. Each colored column is the result of a 6-second probe. The height of the columns indicates the average number of fluorescence counts detected per laser pulse and the color indicate the classification result (the bottom window shows the corresponding color code). The yellow trace is the time evolution of concentration of aerosols having diameters between 1 and 10 µm as measured by an APS. The first vertical dotted line marks the start of the air curtains confining the bioaerosol clouds. At that moment, SR-BioSpectra detected the re-aerosolization of the previous release, an artifact of the chamber. These results were provided by the lidar operator without knowledge of what was disseminated in the chamber and when. Note that the algorithm thresholds were not optimized before obtaining these results which explains some of the artifacts, such as the negative background fluorescent counts (in grey).

The SR-Biospectra beta model was deployed at DRDC Suffield for a period of two weeks to be challenged by well-characterized bioaerosol clouds produced in the lidar-adapted bioaerosol chamber described in subsection 3.1. The campaign was performed in two phases. The first phase involved challenging SR-BioSpectra with BG, EH, MS2 and OVA clouds. For that first phase, all participants knew what aerosols were disseminated and when such clouds were produced in the chamber. Each cloud was 10-m long and was probed from ranges of 30 m or 100 m at night and under different ambient natural lighting. The typical concentrations of these clouds were 100 ACPLA (about 25% ACPLA/ppl

ratio for BG releases and less than 10% for EH releases), between 0.3-0.5 µg/L (OVA releases) and 800-1800 pfu/L (MS2 releases). Figure 5 shows a typical night result obtained during this first phase. From this type of result, the sensitivity is calculated to be better than 40 ACPLA (BG, 25% ACPLA/ppl) at 4 times the standard deviation (standard deviation is measured before the arrival of the bioaerosol cloud).

The second phase of the trial was aimed at assessing the classification capability of the prototype. To achieve this goal, five blind sessions were performed in the lidar-adapted bioaerosol chamber during night time, with SR-BioSpectra positioned at a range of 100 m. The operator had to continuously probe the chamber volume for a period of about one hour during which releases of BG, EH, MS2 or OVA could be done at any time. Then, the operator had to post-process the data collected during these five sessions with the multi-variate algorithm without any information from the referee sensors. Only the spectral data acquired during the first trial phase was made available to the operator to build a resource library of spectral LIF signatures. The correlation with the referee sensors was overlaid only after the operator had delivered his results of the classification process. Figure 6 shows two examples of typical results obtained from these blind releases. Each of the six blind releases (about 10 minutes each) performed during these five sessions was detected successfully within seconds. Over the combined 60 minutes of detected releases, about 80% of the 600 probes (each probe resulting from a 6-second binning) were classified correctly. Of the remaining 20%, only about 1% were incorrectly classified, the other 19% being not classified (assessed as background) or classified as unknown. These classification results were obtained without optimizing the classification algorithm thresholds.

Figure 7 Picture of the BioSense system with the lidar transmitter raised through the roof of the self-sufficient mobile platform. In this demonstration mode, with the help of stabilizing jacks, this system aims to produce geo-referenced maps of aerosol concentration/cross section products of wide areas over 360 degrees in azimuth and +/- 20 degrees in elevation, up to a range of 5 km with a resolution of 10x10 square meters. From this map, having about a minute refresh rate, suspect aerosol clouds are tracked and stared at for about 10 seconds with a spectrally resolved UV/LIF lidar. A multi-variate analysis is performed on the collected spectra, allowing a classification of the detected cloud. By comparing the collected spectra with a library of naturally occurring fluorescing aerosols, obscurants and ultimately, biological agents, different levels of alarms are triggered.

4.2 BioSense

BioSense is a Technology Demonstration Project (TDP) supported by DRDC aiming to demonstrate that a technology based on an eye/skin-safe spectrometric LIF/SWIR lidar scanning/classifying device is able within seconds to detect, map, track and classify bioaerosol threats over a wide area at multi-kilometre distances with a positive detection and false alarm rate compatible with military operational requirements. It is based on a dual emission wavelength monostatic lidar configuration having an f/1.0, 15-cm diameter emitter telescope at the center of an f/1.3, 38-cm diameter collecting telescope, sharing the same optical axis. The lidar emitter uses a 200 Hz PRF laser diode-pumped Nd:YAG laser which can emit alternatively 6 ns pulses of 8 mJ at 1.57 um, by means of an OPO module, and 5 ns pulses of 24 mJ at 355 nm, using non-linear harmonic tripling wavelength crystals. The BioSense system first, while scanning, simultaneously

records the two perpendicularly polarized SWIR components due to elastic scattering from aerosols as a function of the times of flight to build an aerosol concentration/cross section-product map. From this map, suspect aerosol clouds are identified. The system subsequently stares at each suspicious volume for about 10 sec while the UV lidar induces fluorescence which is spectrally detected by a grating-based spectrometer coupled to a gated ICCD. The spectra have a resolution of 3.4 nm over a 360-712 nm spectral interval. Also while staring, a fourth lidar channel records the UV elastic scattering as a function of the time of flight to confirm the presence of the targeted clouds within the gated range interval. Collecting fields of view (FOVs) of about 260 μrad for all lidar channels are obtained using optical fiber tips at the focusing planes of the lidar collector. To maximize the collecting efficiency, this FOV is designed, as a minimum, twice as large as the combined laser divergences and pointing stabilities of the different emitting channels. The lidar transmitter is mounted in an elevation-over-azimuth scanner providing scanning of more than 360 degrees in azimuth and +/- 30 degrees in elevation with less than 1 μrad, 20 μrad and 60 μrad in angular resolution, repeatability and accuracy, respectively. The overall lidar, including the laser and the scanner, is housed in an environmental enclosure employing 2 Air Conditioner units and 2 desiccant modules designed to keep the lidar optics within the operationally required temperature interval and moisture level when the outside temperature and moisture vary from -10 C to 49 C and from 5% to 100%, respectively. The BioSense lidar is integrated on a self-sufficient mobile platform equipped with two sets of stabilizing jacks; one for the vehicle and the other for the BioSense lidar transmitter once mechanically unlocked from the platform. Figure 7 (left) shows the BioSense transmitter module raised through the roof of the dedicated mobile platform with the stabilizing jacks deployed.

The BioSense system also includes controlling software allowing mission planning, deployment, autonomous/manual surveillance, as well as the acquisition of spectral signatures. The mission planning software is based on Digital Terrain Elevation Data (DTED) allowing the operator to select the best position to deploy the BioSense system in order to perform the optimum surveillance of targeted areas of interest. This program, executable a from standard computer before initiating the deployment, allows predefinition of scanning data (elevation/azimuth angular trajectories) which best profiles the targeted areas at optimal heights varying from 5 to 10 meters above ground; reference probing volumes used to spectrally monitor natural background fluorescing aerosol states; the transmission of the atmosphere; and several other parameters to be used during the deployment phase. The deployment software is initiated by first positioning the BioSense system at the pre-defined site. Then, the BioSense scanner reference frame is aligned with the surrounding topography by aiming/firing the lidar transmitter at remote posts equipped with optical aids (retro-reflectors or high reflection surfaces) that have been precisely positioned using a GPS. The objective of this optical alignment is to produce wide-area geo-referenced aerosol maps having a 10x10 square meter or better resolution up to a range of 5 km. After deployment, autonomous surveillance is initiated. The BioSense lidar scans the areas of interest, inverts the lidar equation and produces geo-referenced maps of the aerosol concentration/cross section-products of the areas of interest, with a refresh rate of about one minute. It is also during the initial phase of the surveillance that the inverse of the background aerosol LIF spectral covariance matrix, a key parameter in exploiting the Mahalanobis distance-based classification algorithm, is built from regular background reference LIF spectral probes. If a suspect cloud of aerosols is detected, the BioSense system tracks and stares at it for about 10 sec with the UV LIF channel and triggers different alarm levels by comparing the resulting LIF spectrum with a library containing the fluorescence characteristics of naturally occurring aerosols, obscurants and, ultimately, real agents. The BioSense system also allows the operator to manually probe using the UV LIF lidar channel, both remote air volumes based on third party information and the aerosol in a dedicated lidar aerosol chamber (see section 3.1) to populate the BioSense spectral library during known, well-controlled aerosol releases.

The BioSense system was delivered under contract at the end of July 2011 following four months of intense integration during which most of the hardware related problems were resolved. The system is presently going into preparative trials where the collected raw data are validated. From this raw data, system sensitivity will be estimated. The system will then go through up to 10 weeks of trials in forested, prairie, maritime and urban environments. From the data harvested during these trials, a series of key performance parameters will be evaluated and compared with targeted objectives. Examples of targeted key performance parameters are a sensitivity of 20 ACPLA, a false alarm rate of once per week and the capability of the BioSense system to perform efficient mission planning/deployment and autonomous surveillance over long time periods. The 20 ACPLA sensitivity is measured at 4 times the standard deviation (referring to the signal before dissemination and having a very low level of natural background aerosol fluorescence) at night during releases over a range interval of 10 m located at a range of 1 km with aerosol clouds of BG spores having an average aerodynamic diameter of 3 μm and a 10% ACPLA/ppl ratio. This night time sensitivity is expected to be degraded by a factor of less than 10 during daytime as a result of the narrow FOV lidar transmitter design. We expect to

obtain several answers in the evaluation of these key performance parameters by Spring/Summer 2012 once most of the data gathered during the trial phase have been analyzed.

5. CONCLUSION

A large part of the present effort in developing early warning for aerosolized biological threats over wide areas is done using simulants of real biological agents. This is largely dictated by the highly hazardous properties of these real agents and the great challenge associated with their safe containment once in an aerosol state. However, the necessity of assessing the scattering properties of these specific materials for the successful development of such a capability dictates the construction of a BioSafety Level 3 (BSL3) benchtop bioaerosol chamber. Such a chamber should not only be able to characterize spectral inelastic scattering as produced by LIF technology but also the new and promising lidar-based approaches based on multi-wavelength elastic scattering. There is presently a significant effort to develop such chamber.

It is also important to be aware that the early detection, tracking and classification of aerosolized biological threats over wide areas, even with a high probability and a very low false alarm rate, does not define a complete biological warfare defence suite. The answer to the question ‘what it is’ introduced at the beginning of this paper cannot be completely satisfied with lidar technologies (at least with the present state of advance of this technology). Sampling the suspect material is paramount to obtain a confirmation of the event, the presumptive identification of the threat to initiate efficient medical counter-measures and subsequent forensic investigations. There are different scenarios to rapidly achieve this necessary sampling operation. Some involve using a static array of point sensors. Others are investigating standoff sensors coupled with small/inexpensive UAVs carrying simple air sampling devices. This last approach for a complete defence suite has the advantage of exploiting the fast detection and geo-referenced mapping capability of standoff sensors such as BioSense to direct within seconds a flight plan to a dedicated UAV. This makes it possible, in principle, to sample within minutes the suspect material by flying the UAV through the tracked cloud, bring back the sample (a non-contaminated sampling canister may be dropped at a pre-defined site) to specialized personnel who will initiate presumptive identification through a biochemical process.

DRDC, in partnership with private industry, has progressed significantly towards the development of a complete efficient defence suite against aerosolized biological threats. Improved standoff biodetection system evaluation capabilities have been built, such as the lidar-adapted bioaerosol chamber, the benchtop bioaerosol LIF chamber and calibrated LIF targets. A few tens of ACPLA sensitivity from a 100-meter range has been demonstrated with a short range lidar system, SR-BioSpectra and similar sensitivities at 1-km range are expected to be demonstrated within the next few months with the BioSense system. Also within these next few months, we expect to have a better grasp of the ability of the BioSense concept to achieve geo-referenced wide area/early warning for aerosolized biological threats. There are still significant challenges associated with an efficient sampling procedure for the final confirmation and identification of a biological attack, and the development of a well populated spectral library of natural fluorescing aerosols, obscurants and real agents. These last challenges are presently the object of significant efforts.

REFERENCES

[1] Measures, R. M., [Laser Remote Sensing: Fundamentals and Applications], John Wiley & Sons, Inc., Chap. 7.4, 1984.

[2] Simard, J.-R., Lahaie, P., Buteau, S., Roy, G., Mathieu, P., McFee, J., Rowsell, S., Ho, J. and Lacasse, P., "BioSense Critical Prototype Evaluation (CPE): Planning and analysis considerations," DRDC Valcartier Technical Memorandum TM 2008-301, Unclassified, 67 pages (2008).

[3] Déry, B., "Conception et fabrication d'une chambre à atmosphère contrôlée permettant l'analyse spectroscopique d'aérosols fluorescents," DRDC Valcartier Contract No. W7701-61896, completed March 31st 2009, Unclassified, 59 pages.

[4] Laflamme, C., Simard, J.-R., Buteau, S., Lahaie, P., Nadeau, D., Déry, B., Houle, O., Mathieu, P., Roy, G., Ho, J., Duchaine, C., "Effect of growth media and washing on the spectral signatures of aerosolized biological simulants," Applied Optics, Vol. 50 Issue 6, pp.788-796 (2011)

[5] Simard, J.-R., Roy, G., Mathieu, P., Larochelle, V., McFee, J., Ho, J., "Standoff sensing of bioaerosols using intensified range-gated spectral analysis of laser-induced fluorescence”, IEEE Trans. on Geoscience and Remote Sensing, Vol. 42, No. 4, pp.865-874 (2004)